

Article

Surface and Bulk Plasmon Excitation on Aluminum Surface at Small to High Grazing Angles

Attila Sulyok ^{1,*} and Karoly Tókési ²

¹ Centre for Energy Research, Institute for Technical Physics and Materials Science, P.O. Box 49, H-1525 Budapest, Hungary

² Institute for Nuclear Research (ATOMKI), P.O. Box 51, H-4001 Debrecen, Hungary

* Correspondence: sulyok.attila@ek-cer.hu

Abstract: We present a series of spectra measured by reflected electron energy loss spectroscopy on an aluminum sample using a cylindrical mirror analyzer. The measurements were performed in the energy range between 250 eV and 2000 eV and with various incident angles, including the grazing geometry of an 88° incident angle. The observed spectra were evaluated and decomposed for surface and bulk excitation. The determined surface plasmon excitations were compared to the elastic peak and to the bulk excitation. We found a slight surface plasmon energy shift with altering glancing angles. We show that this shift exists independently from the bulk plasmon interference.

Keywords: surface plasmon; bulk plasmon; grazing incident electron excitations; energy loss spectroscopy



Citation: Sulyok, A.; Tókési, K. Surface and Bulk Plasmon Excitation on Aluminum Surface at Small to High Grazing Angles. *Atoms* **2022**, *10*, 104. <https://doi.org/10.3390/atoms10040104>

Academic Editor: Luca Argenti

Received: 12 July 2022

Accepted: 22 September 2022

Published: 30 September 2022

Publisher's Note: MDPI stays neutral with regard to jurisdictional claims in published maps and institutional affiliations.



Copyright: © 2022 by the authors. Licensee MDPI, Basel, Switzerland. This article is an open access article distributed under the terms and conditions of the Creative Commons Attribution (CC BY) license (<https://creativecommons.org/licenses/by/4.0/>).

1. Introduction

The study of the inelastic scattering of electrons near a surface region and inside the bulk material has a long history. The inelastic scattering phenomenon is important to quantitative surface analysis based on electron spectroscopy techniques, such as x-ray photoelectron spectroscopy (XPS), Auger electron spectroscopy (AES), elastic peak electron spectroscopy (EPES) and reflection electron energy loss spectroscopy (REELS). During the last decades, measurements of the energy loss suffered by fast electrons have been used for determining optical constants. Typical kinetic energies of electrons are 50–300 keV when they are transmitted through thin (500–2000 Å) solid films. The probability of the energy loss is determined by the imaginary part of the dielectric response function $\epsilon(q, \omega)$, which is a function of the frequency ω and the wavenumber q of the electromagnetic disturbance. Raether [1] pointed out that the dielectric properties determined by electron energy loss spectroscopy (EELS) agree well with those obtained by optical methods. At an energy loss above some tens of eV, however, multiple-scattering events become significant, and the measured properties are surface sensitive [2], thereby complicating the extraction of $\epsilon(q, \omega)$.

The excitation of surface plasmons of thin films by fast electrons was first theoretically investigated by Ritchie in 1957 [3]. Two years later, it was observed experimentally by Powell and Swan [4,5]. Since the first observation of surface excitations, there has been a continued interest in developing a method or technique for the clear separation of surface and bulk properties. Even more, in the pioneering work of Ritchie [3], the surface effects were split into two parts. The first one is the result of additional surface modes of the polarization field in the vicinity of the surface, which have a lowered resonance frequency. The second one is the coupling between surface modes and bulk modes near a boundary, which leads to a decrease of the intensity of bulk excitations. Such a depolarization effect is referred to as the Begrenzungs effect. For more details of plasmon theory, see [6]. For the investigation of the surface and bulk contribution, we presented a Monte Carlo simulation of the reflected electron energy loss spectroscopy (REELS) spectra of silver [7]. The simulation was based on the application of the dielectric function formalism [3,8–10],

where both the individual elastic and the inelastic scattering events in the solid were taken into account. In our early Monte Carlo simulations, the simple form of the surface energy loss functions as well as the bulk ones were applied. We showed that for the proper description of the measured REELS spectra, the contribution of the surface losses are significant, especially at low incident energies.

Regarding the energy loss events, we can distinguish between soft and hard collisions. Heavy particles feature the advantage that for projectiles moving parallel to a planar surface, the stopping power resulting from the dielectric response of the surface can be probed without direct (“hard”) collisions. However, since the ion is always attracted towards the surface by its self-image potential, it will suffer a close collision upon impact on the surface. This problem can be avoided using a microcapillary target. This technique has been introduced as a tool to study above-surface processes [11–14]. As an interesting application, we showed that the trajectories that do not undergo charge exchange but come close enough to the walls to suffer a significant stopping power can probe the individual surface loss function of the capillary material.

In this work, the reflected electron energy loss spectra of aluminum are studied experimentally. The backscattered electron energy spectra were measured in reflected mode at an energy range between 250 eV and 2000 eV and at a wide range of incident angles, including the grazing geometry of an 88° incident angle compared to the surface normal. Many authors have studied the combination of surface and bulk losses in various models [1,2]. The absolute intensities of surface and bulk plasmons strongly depend on the primary energy and on the geometrical conditions, such as the angle of incidence of impacting and escaping electrons. Opposite to the bulk losses, the description of surface loss events has not been fully addressed; in particular, the grazing conditions have yet to be determined. We designed a special geometrical arrangement in which the grazing angle of the primary beam is reliably set up. We present and analyze a series of spectra measured by reflected electron energy loss spectroscopy on an aluminum sample using a cylindrical mirror analyzer. Our novel experimental condition makes possible the determination of the surface plasmon energies with an improved accuracy and that allowed the revealing of the energy shift of the surface plasmon.

2. Experimental

Loss spectra were measured on an aluminum layer target that was a 100 nm Al layer evaporated onto an Si wafer. The target was mounted in the UHV condition of 1.0×10^{-9} mbar and cleaned before the measurement by a widely scanned 1 keV Ar ion bombardment.

The novelty of our experimental arrangement is that the specimen in oblique condition results in altering the angle of incidence by changing the azimuthal angle of the specimen. We show this uncommon arrangement in Figure 1. As is visible, the target was mounted at a 45° slope to a sample holder with rotating ability around a vertical axis, as shown in Figure 1. The electron beam of primary electrons was produced by an electron gun from a side position, and it reached the surface in a 150 micrometer spot. The rotation of the sample around its vertical axis provides an easy way of changing the angle of the primary beam relative to the surface plane. Describing this angle, we use the glancing angle (the angle measured from the surface plane) further in this paper, which is complementary to the usual angle of incidence (measured from the surface normal). The observed spectra cover the $1.3\text{--}73.7^\circ$ range of glancing angles. This particular geometry enables us to provide very accurate angular conditions for small grazing cases ($1\text{--}10^\circ$). Because at first a zero-grazing-angle (parallel to the surface) position was determined, the required grazing angle was adjusted by turning the sample away. This setup is less accurate, however, for high grazing angles (above 30°).

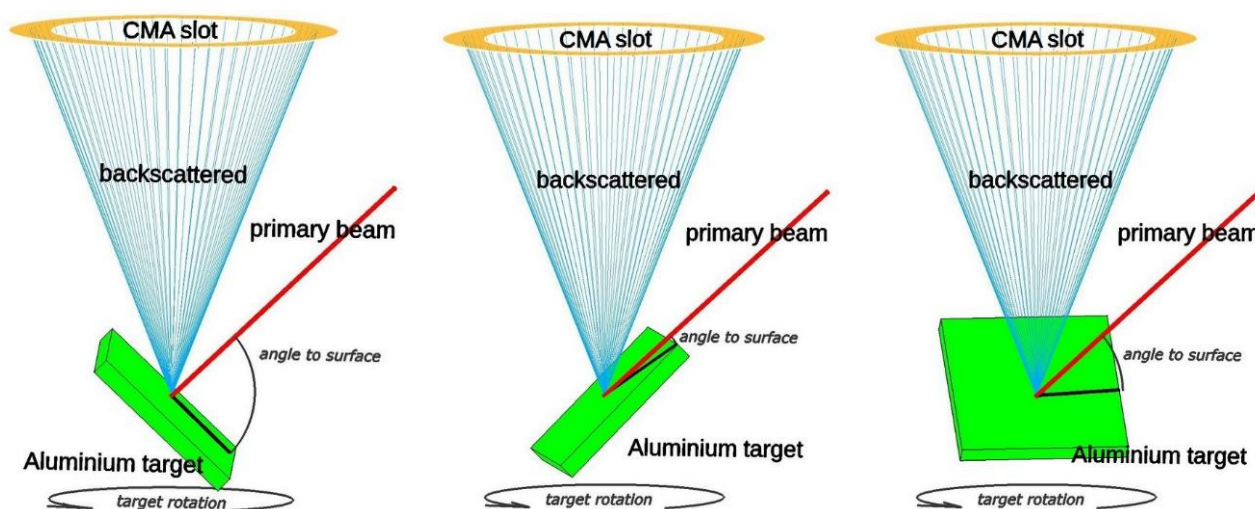


Figure 1. Experimental arrangement of spectrum detection to show the geometrical conditions at a low glancing angle (**left**), at a medium glancing angle (at the **center**), and at a high glancing angle (**right**).

Electron spectra of backscattered electrons were detected by a vertically mounted cylindrical mirror analyzer (CMA), whose ring-shaped entrance slot is marked in yellow in Figure 1. The axis of the sample rotation was adjusted to be identical to the symmetry axis of this cone-shaped detection. Thus, the angular relation to the detector slot did not change with sample rotation, though the cone defined a range of glancing angles for the escaping electrons.

The analyzer itself was a special retarding field CMA (type DESA 150 made by Staib Instrumente GmbH, Langenbach, Germany), with a constant energy resolution over the whole energy range. The energy resolution of measured spectra was limited by the energy width of the primary beam. It was 1.0–1.2 eV, depending on the primary energy. Electron spectra were detected with 0.1 eV steps.

3. Results and Discussion

Aluminum spectra were detected varying excitation energy from 250 eV to 2000 eV and a changing excitation beam of the glancing angle from 1.3° to 73.7° . This resulted in a wide range of surface/bulk intensity ratios, according to the conditions.

To describe the electron backscattering, the events of electron transport that need to be taken into account concern both the primary electrons and the raised secondary electrons. After the primary electrons reach the target, several types of interactions with stochastic relevance start to influence the electron movement. The elastic scattering on the atomic potential produces high angle alteration of the electron path without energy loss (disregarding the tiny energy exchange with the recoil atom). Without elastic scattering, practically no backscattering could be observed, since other interaction events cannot provide enough momentum transfer to the primary electron to result in backscattering. Energy loss processes like ionization loss and plasmon loss are responsible for the alteration of electron energy, though they contribute to the path deviation as well. The multiple occurrences of these inelastic processes result in an energy distribution of electrons that is dependent on the penetrating distance from the surface. A special slice of this distribution that is present at the surface can be observed by external detector and yields the backscattered spectrum. In case of aluminum, the dominant energy loss process is plasmon excitation, including bulk and surface plasmon excitation. These plasmon loss peaks can easily be observed in the neighborhood of the elastic peak (the heap of electrons backscattered without energy loss). With a simple consideration of geometrical conditions, the lowering glancing angle results in

- higher surface plasmon peaks, because the longer path is traveled in the surface region where the surface plasmon is excited;
- lower bulk plasmon excitation, because primary electrons penetrate shallowly and the primary electron is able to lose energy without bulk plasmon excitation.

The strengthening of the surface feature should also reflect the standalone and overlapping multiple plasmon peaks.

For demonstration, two spectra are shown in Figure 2, measured at 1 keV excitation energy with different angles of the excitation beam. The ratio of surface/bulk can be changed back and forth with altering the glancing angle of the excitation beam. The experimental setup allows the varying of the angle of the primary beam only while the escaping electrons traveled on the same paths with the same angles in all cases. This results in some equalization of the ratio. Obviously, an experimental condition where the geometry of escaping electrons can be adjusted too, would provide a more significant change of surface/bulk plasmon ratios.

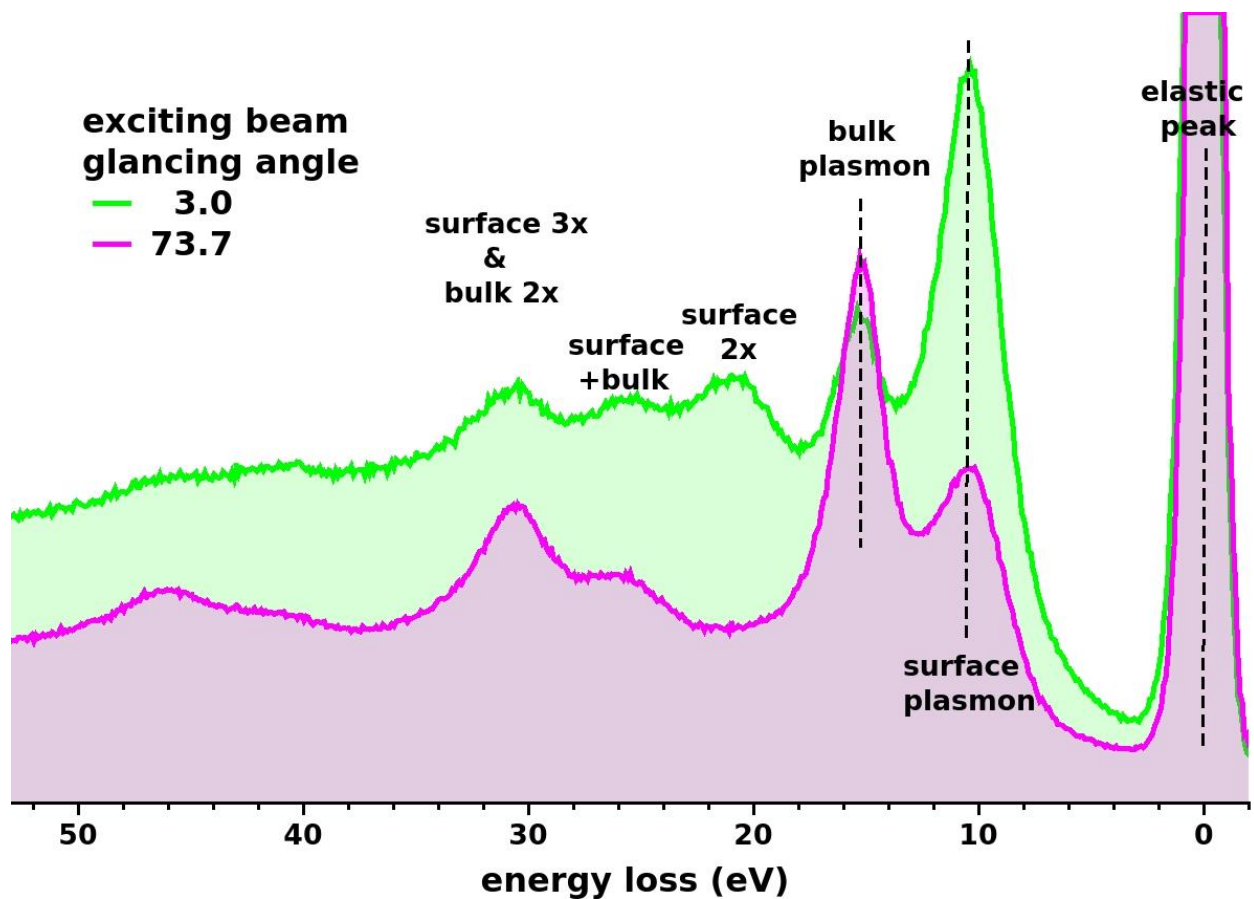


Figure 2. Al loss structure with surface and bulk plasmons excited by 1000 eV primary beam. The excitation angles were 3.0° (purple line) and 73.7° (green line), while the escaping angle was identical. A few identified single and multiple plasmon peaks are denoted.

On the other hand, using the same simple consideration, lowering the energy of primary beam results in

- lower bulk plasmon excitation (because of lower penetration of primary electrons);
- larger surface plasmon excitation (because of larger cross section of surface plasmon excitation).

The lower bulk and higher surface excitation has a consequence for single and multiple plasmons.

Figure 3 shows two spectra detected at a moderate glancing angle of 32.3° at different energies. The ratio of surface/bulk plasmon losses can be varied in a wide range by adjusting the excitation energy.

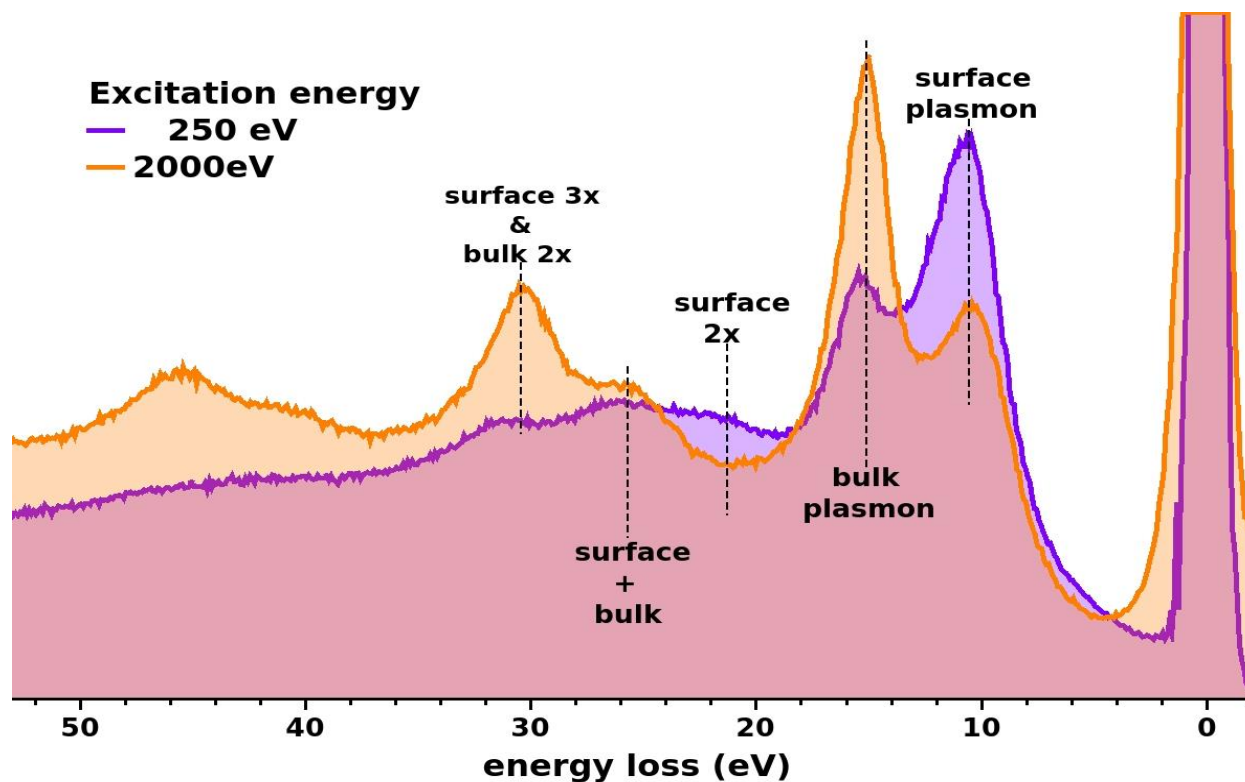
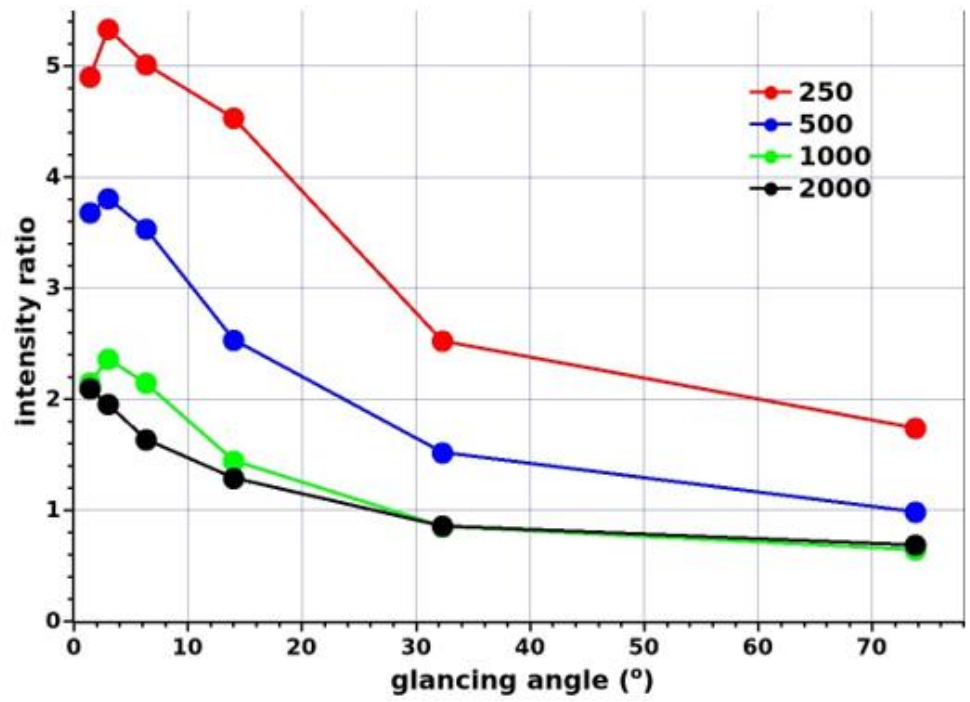


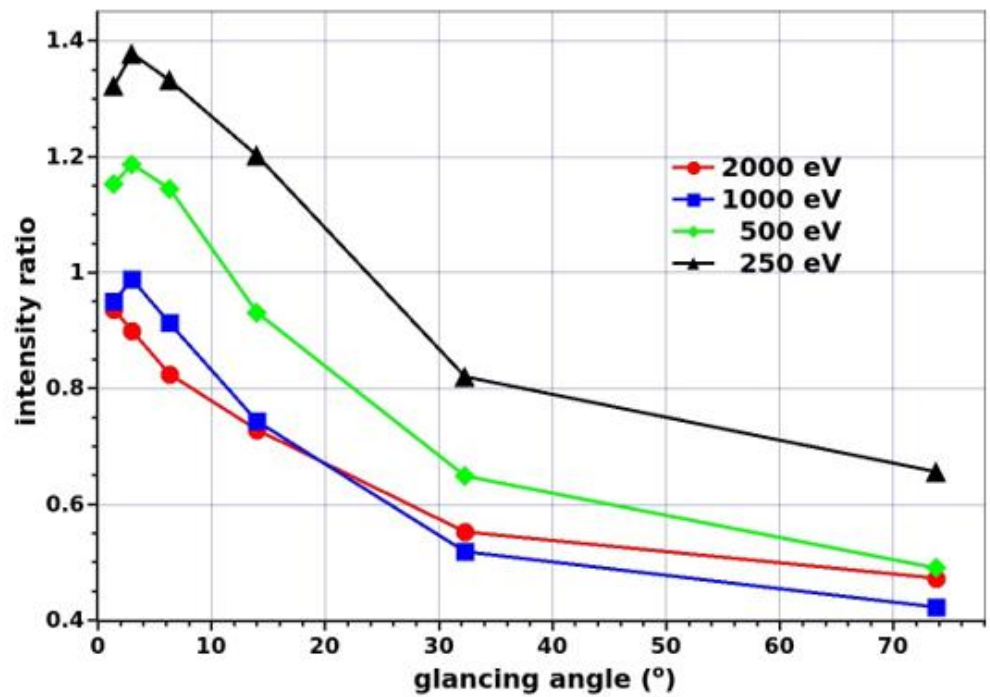
Figure 3. Al loss structure with surface and bulk plasmons excited by primary beam with 32.3° glancing angle. The energy of the primary beam was 250 eV (blue line) and 2000 eV (braun line). Triple surface plasmon peak overlaps with double bulk plasmon peak. Other multiple losses are not denoted.

The evaluation of the measured spectra took place by determining the contributions of elastic peak, single surface excitation, and single bulk excitation. Multiple excitations were also determined, however, they are not presented here because their intensity could be calculated with less certainty. The spectrum was decomposed by fitting these components with a Gaussian-Lorentzian shape. As a result, the fit included an optimized peak position, intensity, width, and asymmetry. The intensity of a peak is defined by the area of the peak. For characterizing the surface excitation, the surface plasmon peak/elastic peak ratio as well as the surface plasmon peak/bulk plasmon peak ratio were calculated. These ratios are shown in Figure 4a,b, respectively, for the entire observed ranges.

According to our measurements, at low energies and grazing incident angles, the surface plasmon intensity can be larger than the elastic peak intensity. The measurement of the energy loss spectra of Al revealed a barely studied feature. The energy of the surface plasmon slightly shifted with the variation of the incident angle. The loss spectra measured with 250 eV excitation energy at different glancing angles are shown in Figure 5a. It clearly shows the shift of the surface plasmon peak, that is, the change of the surface plasmon energy, as the larger glancing angle beam generates surface loss with larger energy.



(a)



(b)

Figure 4. Surface plasmon relative intensity on Al surface measured against glancing angle for some primary energies. (a) (upper part): Surface plasmon/elastic peak ratio. It is normalized to the elastic peak intensity using an integrated area for both. (b) (lower part): Surface plasmon/bulk plasmon ratio.

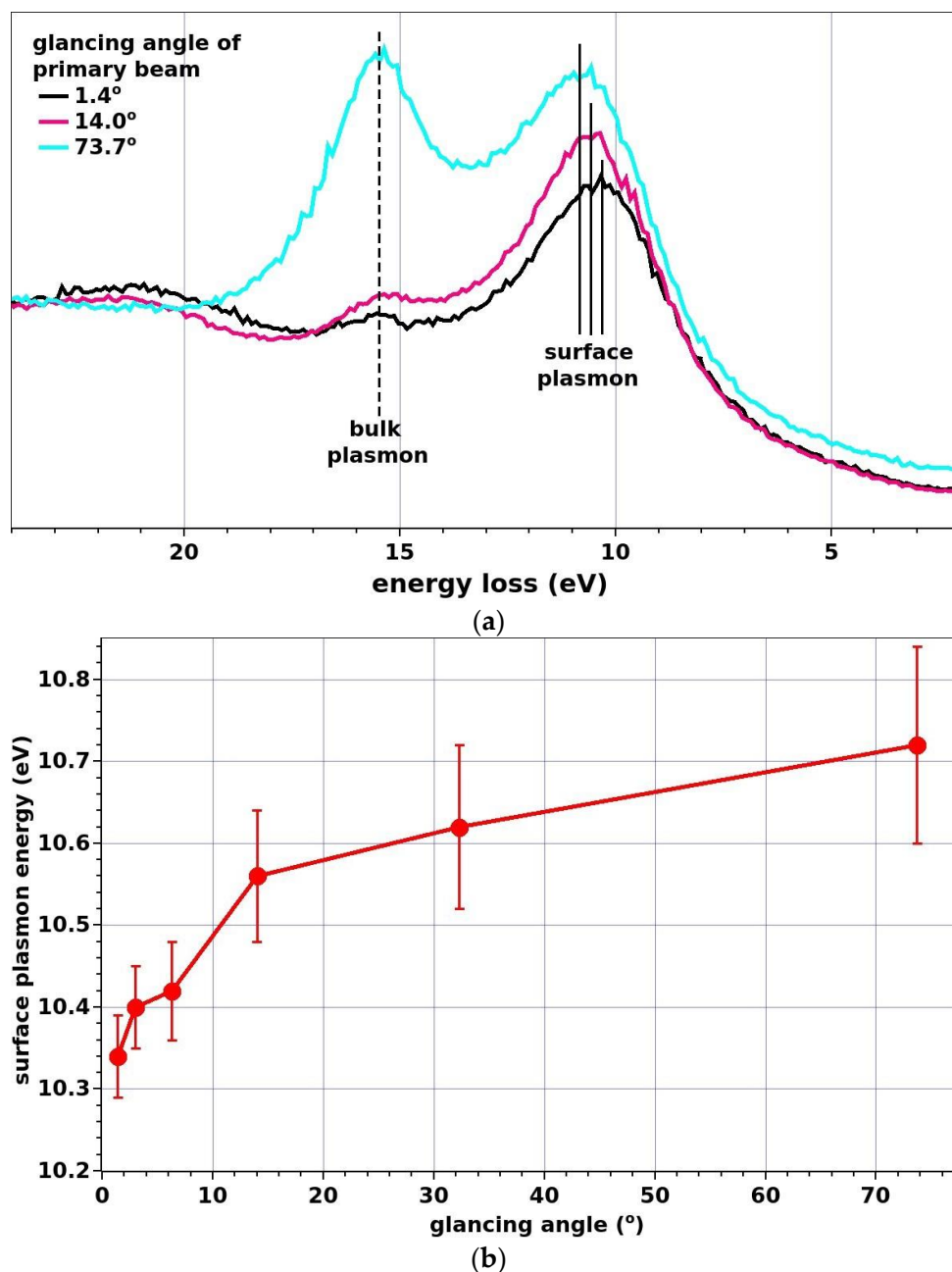


Figure 5. The change of surface plasmon energy with glancing angle, measured on Al at 250 eV. (a) (upper part): The visible shift of surface plasmon peak position shows the changes of surface plasmon energy on the Al surface with altering glancing angle of primary beam. Spectra are normalized for comparable size for better visualization. (b) (lower part): Calculated surface plasmon energy versus glancing angle of exciting electron beam, including the estimated error bars. The calculated energy values were derived from the measured spectra with peak fitting.

Because this is a new experimental finding for a well-studied topic, further explanation is necessary regarding our findings. Though the energy shift is a relatively small change (a few 100 meV) of a wide (4 eV) peak, it is more significant at low grazing angles. Plasmon measurements are mostly carried out at higher grazing angles, where the energy shift is small (below 100 meV). Detection is difficult because the surface plasmon peak overlaps with the bulk plasmon peak. We introduced, however, an experimental novelty that made possible the determination of the energy shift with reasonable accuracy. The measurement at low grazing angles improved the accuracy by twofold:

- the low grazing angle resulted in higher energy shift (over 300 meV) of the surface plasmon peak, which was easier to identify;
- the low grazing angle resulted in larger surface plasmon and smaller bulk plasmon peaks, and thus the influence of bulk to the surface plasmon is less disturbing (see black and purple lines in Figure 5).

Obviously, the actual energy of the surface plasmon is not identical to the position of the visible peak in the loss spectrum. The correct surface plasmon energies are calculated from the measured spectra and are shown in Figure 5b. The energy values are derived from the decomposition of loss spectra by peak fitting, which is much more precise (see details below) than reading the peak position. Figure 5b shows that the energy of the surface plasmon changes almost 0.4 eV, while the excitation angle changes from 1.4° to 73.7° .

To conduct analyses of the possible errors made in this decomposition, one needs to consider that the visible spectrum is a sum of several loss processes that also provide contributions at the position of the surface plasmon. If these other losses have a slope at the location of the surface plasmon, it may shift the position of the visible peak. The most significant effect is the bulk plasmon loss, which indeed provides some slope at the surface plasmon. Consequently, the larger the glancing angle, the larger the contribution of the bulk plasmon, which provides a larger shift of surface plasmon toward higher energies. The evaluation of the measured spectra showed that this bulk plasmon-induced shift of the visible peak is far less than the detected shifts. The largest bulk plasmon-induced shift of the visible peak is obtained at the highest glancing angle (73.7°), when the bulk contribution is the largest. In this case, the bulk plasmon-induced shift of the visible peak is 0.11 eV, that is, the position of visible peak is shifted from 10.72 eV to 10.83 eV due to the presence of bulk plasmon. This 0.1 eV is much smaller than the observed 0.5 eV difference for the changing glancing angle. For lower glancing angles, the bulk plasmon-induced shift of the visible peak quickly diminishes and thus becomes less disturbing. Thus, we can state that the shift of the visible surface plasmon peak cannot be explained by the increasing bulk contribution; instead, it basically results from the changing energy of the surface plasmon.

It must be noted here that the experimentally observed surface plasmon is a sum of all the surface losses generated in the actual geometrical condition. The exciting beam had a definite glancing angle and was controlled by sample rotation, according to the graph of Figure 1. The escaping electrons had identical paths toward the detector, disregarding the excitation condition and covering a range of glancing angles. The detector has a ring-shaped slot with an axis of 45° glancing angle and about $\pm 22^\circ$ cone width. Thus, the detected surface plasmon heap has contributions from the controlled angle incoming electrons and the fixed-ranged escaping electrons. These contributions have slightly different plasmon energy, however, and cannot be separated because of their great overlapping. This may explain our finding that the shape of the surface plasmon obtained by decomposition is not an ideal Lorentzian, but still has a weak asymmetry (see Figure 6). For better visibility, the ideal (symmetrical) shape of the surface plasmon is drawn by a dotted line. The asymmetry is the most significant for the single surface plasmon shape, though the multiple losses are also influenced (not shown in Figure 6).

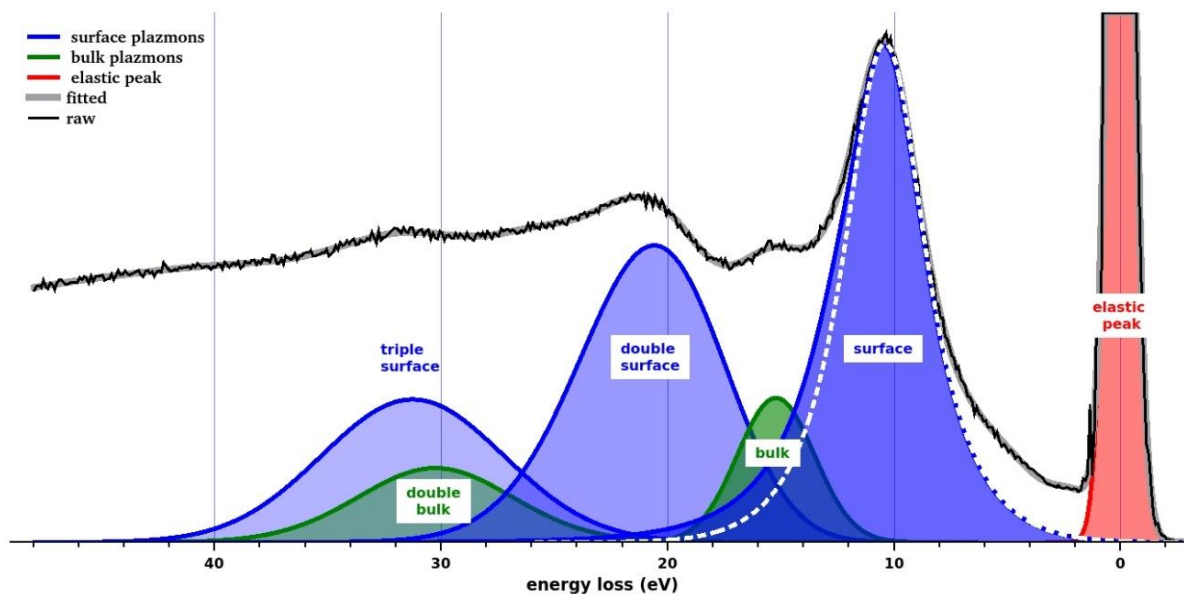


Figure 6. Decomposition of loss spectra observed at 3° glancing angle with 250 eV primary energy. Only main components of surface and bulk plasmons are drawn. Asymmetric shape of surface plasmon is visible at the single surface loss peak in comparison to an ideal plasmon shape (dotted line).

4. Summary

The multiple surface and bulk excitations are studied experimentally by electron impact on aluminum samples. The reflected electron energy loss spectroscopy measurements were performed using a cylindrical mirror analyzer-type electron spectrometer at an energy range between 250 eV and 2000 eV and at a wide range of incident angles. The highlight of our recent investigations was that our measurements were also performed at grazing incident angles such as an 88° incident angle compared to the surface normal. The observed electron energy loss spectra were evaluated and decomposed into surface and bulk excitation. We obtained a series of single and multiple surface and bulk plasmon losses in the measured spectra. The measurement of grazing angles resulted in improved accuracy in determining surface plasmon energy. We found surface plasmon energy shifted with altering glancing angles. We showed that this shift exists independently from bulk plasmon interference.

Author Contributions: Conceptualization K.T.; methodology A.S.; resources and data acquisition A.S.; software and analysis A.S.; visualization A.S.; writing the original draft, A.S. and K.T.; review and editing, A.S. and K.T. All authors have read and agreed to the published version of the manuscript.

Funding: This research received no external funding.

Data Availability Statement: Can be obtained from the authors on request.

Conflicts of Interest: The authors declare no conflict of interest.

References

1. Raether, H. *Springer Tracts in Modern Physics*; Springer: Berlin/Heidelberg, Germany, 1965; Volume 28.
2. Tökési, K.; Kövér, L.; Vaga, D.; Tóth, J. Effects of surface loss in REELS spectra of silver. *Surf. Rev. Lett.* **1997**, *4*, 955. [[CrossRef](#)]
3. Ritchie, R.H. Plasma losses by fast electrons in thin films. *Phys. Rev.* **1957**, *106*, 874. [[CrossRef](#)]
4. Powell, C.J.; Swan, J.B. Origin of the characteristic electron energy losses in aluminum. *Phys. Rev.* **1959**, *115*, 869–875. [[CrossRef](#)]
5. Powell, C.J.; Swan, J.B. Origin of the characteristic electron energy losses in magnesium. *Phys. Rev.* **1959**, *116*, 81–83. [[CrossRef](#)]
6. Arista, N.R.; Gervasoni, J.L.; Segui, S.; Villo-Perez, I.; Barrachina, R.O. Plasmon excitation by charged particles in solids, surfaces, and nanostructures: Following the trail of R.H. Ritchie. *Adv. Quantum Chem.* **2019**, *80*, 271.
7. Gong, J.M.; Yang, L.H.; Tökési, K.; Ding, Z.J. Surface and bulk plasmon excitations of silver by electron impact. *Eur. Phys. J. D* **2019**, *73*, 24.
8. Ritchie, R.H.; Marusak, A.L. The surface plasmon dispersion relation for an electron gas. *Surf. Sci.* **1966**, *4*, 234. [[CrossRef](#)]

9. Ding, Z.J.; Shimizu, R. Monte Carlo study of backscattering and secondary electron generation. *Surf. Sci.* **1988**, *197*, 539.
10. Ding, Z.-J.; Shimizu, R. Inelastic collisions of kV electrons in solids. *Surf. Sci.* **1989**, *222*, 313. [[CrossRef](#)]
11. Yamazaki, Y.; Ninomiya, S.; Koike, F.; Masuda, H.; Azuma, T.; Komaki, K.; Kuroki, K.; Sekiguchi, M. Stabilized hollow atoms (ions) produced with multiply charged ions passed through microcapillaries. *J. Phys. Soc. Jpn.* **1996**, *65*, 1199. [[CrossRef](#)]
12. Ninomiya, S.; Yamazaki, Y.; Koike, F.; Masuda, H.; Azuma, T.; Komaki, K.; Kuroki, K.; Sekiguchi, M. Stabilized hollow ions extracted in vacuum. *Phys. Rev. Lett.* **1997**, *78*, 4557. [[CrossRef](#)]
13. Tökési, K.; Wirtz, L.; Burgdörfer, J. Interaction of highly charged ions with microcapillaries. *Nucl. Instr. Meth. B* **1999**, *154*, 307. [[CrossRef](#)]
14. Tökési, K.; Wirtz, L.; Lemell, C.; Burgdörfer, J. Charge-state evolution of highly charged ions transmitted through microcapillaries. *Phys. Rev. A* **2000**, *61*, 020901. [[CrossRef](#)]